A&A 494, 845–855 (2009)
DOI: 10.1051/0004-6361:200810384

Astronomy & Astrophysics

Galaxy clusters in the CFHTLS⋆

II. Matched-filter results in different passbands

L. F. Grove[1,⋆⋆], C. Benoist[2], and F. Martel[2]

[1] Dark Cosmology Centre, Niels Bohr Institute, University of Copenhagen, Juliane Maries Vej 30, 2100 Copenhagen, Denmark
e-mail: lisbeth@dark-cosmology.dk
[2] Observatoire de la Côte d'Azur, Laboratoire Cassiopée, BP 4229, 06304 Nice Cedex 4, France

Received 13 June 2008 / Accepted 7 November 2008

ABSTRACT

Aims. We investigate the gain of added leverage and completeness of the constructed cluster catalogue, of applying the matched-filter detection algorithm to multiple passbands. In particular, we investigate the gain from having both i'- and z'-band data available when searching for galaxy clusters at $z \gtrsim 1$.
Methods. We applied a matched filter detection method to the CFHTLS r'- and z'-band data of the four Deep fields and compared the cluster catalogues with the one extracted from the i'-band data presented in a previous paper. We also applied the matched filter to the Deep fields but with the limiting magnitudes appropriate for the much larger Wide survey in order to understand the best combination of i'- and z'-band depth for the most efficient cluster searches based on this algorithm.
Results. The density of clusters identified in the Deep r'- and z'-band catalogues are 36 and 80 per square degree, respectively. The estimated densities of false detections are 12 and 20 per square degree in the two bands. We find that the recovered properties are in good agreement between the different bands and also that the efficiency of each band is consistent with the expectations based on the shift of the 4000 Å break through the filters. When comparing r'- and i'-band, we do not find any significant additions to the i'-band catalogue. On the contrary, we find a large number of high redshift detections in the z'-band not in i'. These detections add ∼60% to the number of high-redshift detections in the i'-band.
Conclusions. We conclude that, for cluster searches to redshifts ≳1, it is important to include sufficiently deep data redward of the i'-band, which in this work is provided by the z'-band coverage. The combination of catalogues extracted from two different passbands does not provide a cluster sample with greater purity.

Key words. methods: data analysis – surveys – galaxies: clusters: general – cosmology: large-scale structure of Universe

1. Introduction

Clusters of galaxies are important tools in observational cosmology (e.g. Borgani et al. 2001; Rosati et al. 2002). They are the largest relaxed structures in the Universe with both their properties and evolution tightly connected to the cosmological parameters and to the physics of structure formation. However, to fully understand structure evolution and constrain cosmological parameters, large, well-understood samples are required. Therefore, in recent years a number of automatic and objective cluster searches have been or are being carried out. Currently, the main searches are being carried out in X-rays or at optical wavelengths, but soon searches based on the Sunyaev-Zel'dovich effect are expected to start contributing. The X-ray searches have the great advantage that the contamination rate is low, however, covering the large areas to the necessary depth needed for building up statistical samples over a wider redshift range is very time consuming. Some of the most widely used X-ray surveys originate in the ROSAT data. Only one survey, the ROSAT Deep Cluster Survey, reaches cosmologically relevant redshifts. This survey identified clusters in the redshift range $z \lesssim 0.8$ with a density of ∼3.3 per square degree over 48 square degrees (Rosati et al. 1998). In the optical, the ongoing searches are based on large areas and deep data, appropriate to search large volumes at a range of redshifts (e.g. RCS2[1] and CFHTLS[2]). Among the largest and deepest searches are the Red-sequence Cluster Survey (RCS), which led to the identification of clusters with $0.35 \lesssim z \lesssim 0.95$ at a density of 13.3 per square degree over ∼72 square degrees (Gladders & Yee 2005). Other surveys have reached slightly higher densities ∼15−20 per square degree covering slightly larger redshift intervals of about $0.2 \lesssim z \lesssim 1.2$ (e.g. Postman et al. 1996; Scodeggio et al. 1999).

A number of automatic cluster identification methods have been developed for detecting clusters in optical data. The first objective methods developed were based on detections in a single passband and on applying a maximum likelihood algorithm indexed by the redshift (e.g. Postman et al. 1996; Olsen et al. 1999a; Kepner et al. 1999). These methods modelled the clusters based on typical luminosity functions and radial profiles. More recently, methods based on two (e.g. Gladders & Yee 2000; Koester et al. 2007) or more passbands (e.g. Goto et al. 2002; Miller et al. 2005) have been used to identify clusters. Such methods improve the ability to disentangle chance alignments, but they also rely on their own assumptions, such as the presence of the colour-magnitude relation of early type galaxies (e.g.

⋆ Tables 4 and 5 are only available in electronic form at the CDS via anonymous ftp to cdsarc.u-strasbg.fr (130.79.128.5) or via http://cdsweb.u-strasbg.fr/cgi-bin/qcat?J/A+A/494/845
⋆⋆ Previously, L. F. Olsen.

[1] http://www.rcs2.org
[2] http://www.cfht.hawaii.edu/Science/CFHLS

Bower et al. 1992; Stanford et al. 1998; de Propris et al. 1999). Each of the detection methods have their own biases and selection effects depending on their specific assumptions. A good understanding of these effects is essential for constraining the structure-growth function based on cluster experiments. In principle, such an understanding is best addressed statistically from the analysis of realistic mock catalogues. However, the difficulty in reproducing the galaxy properties within forming clusters in simulations covering a cosmological volume, leads to the necessity of also investigating biases of cluster finders by direct comparisons on real data.

The Sloan Digital Sky Survey (SDSS) data with their large area and multi-colour coverage, as well as complementing spectroscopic information, have recently provided an important testbed for a number of optical cluster detection methods at low redshifts (e.g., Kepner et al. 1999; Kim et al. 2002; Goto et al. 2002). Thorough comparisons between the different methods have been carried out by Kim et al. (2002); Goto et al. (2002) and Bahcall et al. (2003). These comparisons show that, not surprisingly, there are always differences between the various catalogues, some of which are caused by the different ways the parameters, such as for example richness, are estimated. The SDSS data are sufficient for detecting clusters to at most intermediate redshifts ($z \sim 0.5$). At higher redshifts only smaller data samples have been available, such as the KPNO/Deeprange survey by Postman et al. (2002) and the ESO Imaging Survey (Olsen et al. 1999a,b; Scodeggio et al. 1999). Recently, the Red sequence Cluster Survey by Gladders & Yee (2005, RCS) covering 100 square degrees has been achieved thus starting to probe large volumes to high redshift. However, a detailed comparison of the efficiency of different methods at high-z has yet to be carried out.

For detailed comparisons between different methods, wide, deep, and preferentially multi-passband homogeneous surveys are required in order to provide the necessary data for a number of different detection methods. The design of the Wide survey of the Canada-France-Hawaii Telescope Legacy Survey (CFHTLS) provides a data set that is particularly well-suited to carrying out such studies. This survey is currently underway and is planned to cover $\sim$ 170 square degrees in 5 passbands spread in 4 patches with limiting magnitudes up to $25^{\rm m}$. It will provide the necessary ground for building a large, well-controlled cluster candidate sample at redshifts $z \lesssim 1.3$, derived from a set of different search techniques using the spatial and/or photometric properties in one or more passbands. Such catalogues will allow us to accurately test the $z > 0.5$ component of the cluster distribution. Using automatic search techniques will allow us to build selection functions for each of our independently extracted catalogues. A careful comparison between the various independently extracted cluster samples will allow us to understand the additional difficulties in detecting clusters at successively higher redshifts, as well as improve our knowledge about clusters at these redshifts. Combining the catalogues from several searches we will create a robust cluster sample well-suited to both cosmological and galaxy evolution studies.

Based on the CFHTLS Deep data, several optical cluster finders have already been applied including the i'-band matched filter (Olsen et al. 2007, hereafter Paper I), photometric redshift slicing (Mazure et al. 2007), and weak lensing (Gavazzi & Soucail 2007). In this paper we compare the results of applying the matched filter detection method to different passbands, thereby discussing the benefits of having independent cluster catalogues for gaining leverage of individual systems, and to complement each other at redshifts where the bluer passbands become less efficient. In Paper I we described our implementation of the matched filter and its application to the CFHTLS i'-band catalogues. Here we extend this work to the r'- and z'-bands with the main aim of investigating the added value of the different bands. We also investigate the outcome expected from the CFHTLS Wide in terms of depth and completeness of the cluster search. The paper is structured as follows. In Sect. 2 we describe the galaxy catalogues used as the basis for our search. In Sect. 3 we give an overview of the detection method and describe the parameter settings based on simulations, as well as the selection function for each passband. In Sect. 4 we present the new cluster candidate lists for the r'- and z'-band and compare them with that of the i'-band presented in Paper I. In Sect. 5 we discuss the added value of the new passbands. In Sect. 6 we discuss the expected outcome of the CFHTLS Wide survey in terms of depth of the extracted cluster catalogues and the optimum combination of depth in the i'- and z'-band for obtaining the most complete cluster sample based on the matched filter algorithm also at high redshift. In Sect. 7 we summarise the paper.

Throughout the paper we use a cosmological model with $\Omega_{\rm m} = 0.3$, $\Omega_\Lambda = 0.7$, and $H_0 = 75$ km s^{-1} Mpc^{-1} [3].

Table 1. Characteristics of the released data in the r'- and z'-bands of the T0003 Terapix release.

Passband	r'	z'
Exposure time [h]	8.8–20.2	10.1–20.1
Seeing [arcsec]	0.88–0.94	0.83–0.88
Magn. at 80% completeness	24.3–25.8	24.4–24.7

2. Galaxy catalogues

Our implementation of the matched filter algorithm treats one passband at a time, thus the basic input is the single passband galaxy catalogues. The basic source catalogues in the r'- and z'-bands are the ones provided by the Terapix team as part of the CFHTLS release T0003 in February 2006[4]. For the i'-band we continue to use the ones from the T0002 release as in Paper I to facilitate the comparison to the previous work. The characteristics of the released data in the r'- and z'-bands are summarised in Table 1 given as ranges for the four deep fields considered here.

Starting from the release catalogues, we apply a star-galaxy separation based on the locus of the objects in a half-light radius versus i'-magnitude diagram, where the stars are clearly separated from the galaxies at magnitudes $i' \lesssim 21 - 22$. As in Paper I we applied a correction for Galactic extinction based on the Schlegel et al. (1998) maps and used the masks created for the i'-band images to exclude false detections. For these post-processed catalogues, we show the differential number counts in Fig. 1 for each of the four Deep fields considered in this paper. It can be seen that the number counts for the four fields are consistent. The vertical dotted lines mark the limiting magnitudes applied for this work which for the r'-band is $r' = 25.0^{\rm m}$ and for z'-band $z' = 24.5^{\rm m}$.

3. Cluster detection

3.1. The matched-filter procedure

Our cluster detection procedure was described in detail in Paper I. It was based on the matched-filter technique (e.g.,

[3] We use $h_{75} = \frac{H_0}{75 \text{ km/s/Mpc}}$.

[4] http://terapix.iap.fr/rubrique.php?id_rubrique=208&PHPSESSID=68382a75ec8b2e8b05a4e0dd5371e838

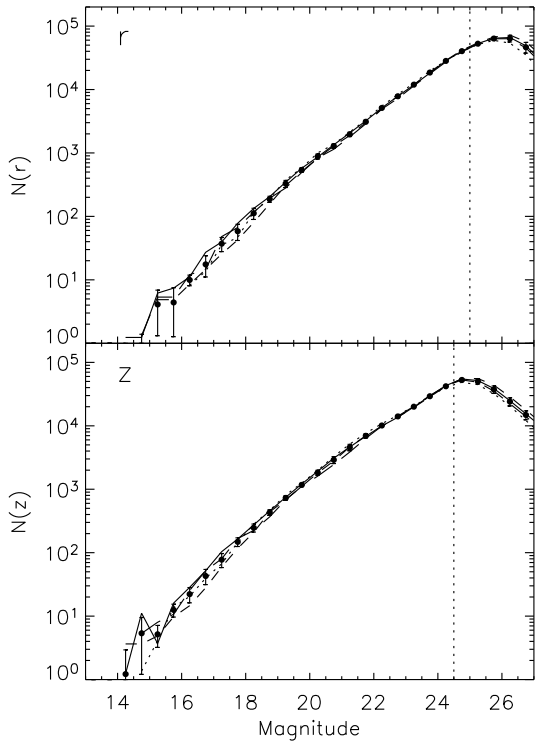

Fig. 1. Average galaxy number counts (filled dots with error bars) for the four Deep fields in the r'- and z'-band as indicated in each panel. The number counts for the individual fields are shown as follows: D1 – solid line; D2 – dotted line; D3 – short-dashed line; and D4 – long-dashed line. The vertical dotted lines denote our adopted magnitude limit for the present analysis.

Postman et al. 1996) as it was implemented for the ESO Imaging Survey (Olsen et al. 1999a) with some additional improvements. Here we only summarise the main steps and our choice of input parameters for the present work.

The matched-filter technique is a maximum likelihood analysis with the following steps:

1. creation of a filter based on an assumed cluster galaxy luminosity function and radial profile;
2. creation of likelihood maps for a series of redshifts;
3. detection of significant peaks;
4. cross-matching of peaks for different redshifts;
5. creation of likelihood curves and identification of the redshift of maximum likelihood used for defining the cluster properties such as redshift and richness.

For constructing the filter, we used the Schechter luminosity function (Schechter 1976) and a Hubble radial profile. The main parameters are listed in Table 2, and are the Schechter magnitude, M^* and the faint end slope of the luminosity function, both taken from Popesso et al. (2005) and converted to our cosmology, and the core- and cutoff radii for the radial profile. As discussed below, the peak detection parameters were set based on a balancing of the fraction of false detections and the recovery rate, as was also done in Paper I for the i'-band. Finally, only detections found in at least two consecutive redshift shells were considered.

3.2. Simulated galaxy catalogues

To balance the number of false detections with the recovery rate, we created a set of simulated background catalogues

Table 2. Detection and filtering parameters for building the cluster catalogues.

Parameter	Value
Filter	
Core radius, r_c	$0.1\,h_{75}^{-1}$ Mpc
Cut off radius, r_{co}	$1.0\,h_{75}^{-1}$ Mpc
Faint end slope of LF, α	–1.15
Schechter magnitude, M_r^*	–21.97
Schechter magnitude, M_z^*	–22.48
Likelihood maps	
Pixel scale	$0.5r_c$ = 21.6–8.5 arcsec
z-interval, r'-band	0.2–1.0, $\Delta z = 0.1$
z-interval, z'-band	0.2–1.3, $\Delta z = 0.1$
Peak detection	
Threshold	3.5σ
Minimum area	$\sim\pi\,(r_c(z)/2)^2 \sim 4$ pixels
A posteriori filtering	
Minimum number of shells	2

reproducing the first and second order statistics of the clustering properties of the galaxy distribution. In Paper I we described the procedure used for a single passband for obtaining catalogues resembling the data. There we created 20 simulated background catalogues with an area of 1 square degree each matching the i'-band properties. Those catalogues were used here as the basis for creating the r'- and z'-band, keeping the positions but assigning random r'- and z'-magnitudes according to the magnitude dependent colour distributions. The clustering of the constructed catalogues has been confirmed to resemble that of the data.

To estimate the recovery rate, we added clusters resembling the model cluster. For this purpose we again used the 3360 clusters created in the i'-band in Paper I and applied a redshift dependent colour correction to get the equivalent clusters in r'- or z'-band. We used the colour correction for a non-evolving elliptical galaxy to match the choice in Paper I of using the same k-correction for all galaxies in the cluster, thus for the moment disregarding the effects of variations in galaxy types. The effects of these variations will be discussed in a forthcoming paper where we discuss the selection funcion based on N-body simulations.

3.3. Detection parameters

Our matched filter detection procedure is applied to one band at a time. The data from different passbands are treated independently following the same procedures as in Paper I. The most important parameters for setting up the peak detection are the minimum accepted area and the detection threshold. The two parameters are not independent, since a larger threshold leads to smaller areas and vice versa. In Paper I we estalished that a minimum area of $\sim\pi(r_c/2)^2$ is necessary for achieving a good completeness at high redshifts. It was also found that a number of high redshift X-ray detected systems were only included if the detection threshold was set to 3.5σ. With these settings we found that the fraction of false detections is ~30%. Here we aim at a similar noise fraction. Below, the cross-matching between the different catalogues will be used to assess their relative completeness.

Table 3 gives the estimated frequency of false detections for the r'- and z'-band catalogues and compares these to the one in i'-band for the chosen minimum area and different detection thresholds. From the table it is, as expected, clear that the highest thresholds give the smallest fraction of false positives. However, this also leads to the lowest completeness of the cluster

Table 3. The estimated fraction of false-positives for each of the three passbands using a minimum area of $\sim\pi(r_c/2)^2$ and different detection thresholds.

Det.Thresh.	r'	z'	i'
2.0σ	0.61	0.70	0.73
2.5σ	0.62	0.60	0.69
3.0σ	0.45	0.44	0.52
3.5σ	0.33	0.26	0.32
4.0σ	0.18	0.13	0.18
4.5σ	0.11	0.07	0.09
5.0σ	0.07	0.04	0.06

catalogues and is therefore undesirable. It can be seen that the fraction of false positives do not differ a lot between the different passbands for a given threshold, and thus in all cases we decide to use 3.5σ for the detection threshold. Curiously, the fraction of false detections in the z'-band is at high detection thresholds always lower than in the other bands. The reason for this is not clear, but may be related to a better detection efficiency at high redshift and thus more real detections in the catalogue.

In Fig. 2 we show the redshift distribution of the detections in the r'- and z'-catalogues including the estimated number of false detections. There it can be seen that in both cases the false detections are found in roughly equal number at all redshifts, except that there is a slight indication of a peak at the lowest redshift for the r'-band. The figure also shows the richness distributions. Not surprisingly, the fraction of false positives increases for lower richness.

3.4. Recovery rate

Having decided on the detection threshold and minimum area we investigated the recovery rate as function of redshift and richness. We covered redshifts from $z = 0.2$ to 1.3 and richnesses in the range $\Lambda_{\rm cl} = 10{-}300$. These richnesses correspond to systems of richness class $R < 0$ up to $R \sim 4$. We used the simulated catalogues described above starting from the i'-band catalogues correcting the magnitudes to r'- or z'-band, respectively, and identify systems in these catalogues. This method is equivalent to building clusters for each passband following the Schechter luminosity function also used for constructing the filter as was the procedure for the i'-band; hence the determined recovery rate can be compared directly between the different catalogues.

Figure 3 shows the recovery rate as determined for both bands and compares them with the one found for the i'-band in Paper I. For each band we show the recovery rate for four richness classes starting at poor groups up to very rich clusters as detailed in the figure caption. The cutoff in each passband is related to the shifting of the 4000 Å break out of the filter, which strongly depletes the catalogue for detectable cluster members. For the r'-band, this effect already sets in for the poor clusters at $z \sim 0.5$, while the richer systems are detected with good completeness up to $z \sim 0.9$. For the z'-band the poor systems start to be significantly affected at $z \sim 0.8$ and the rich systems only drop significantly at $z \sim 1.1$. For comparison we also show the i'-band results that can be seen to be intermediate but only slightly shallower in terms of recovery rate than the z'-band catalogue for these idealized cases.

Being able to detect a cluster is obviously the most basic recovery property, however it is also important to know how reliably the parameters are recovered. To investigate this, we studied the offsets in redshift and richness between the input values and matched-filter estimates as was done for the i'-band in Paper I. We find a similar trend towards overestimating the redshift for the most nearby systems, while at high-z we find an underestimate. The offsets in richness are consistent with this picture showing also an overestimate at low-z and an underestimate at high-z. The reason for this is that the $\Lambda_{\rm cl}$-richness gives the equivalent number of L^* galaxies and thus an overestimated redshift gives a fainter estimated apparent Schechter magnitude, which leads to overestimating the richness. The effect is opposite for the underestimated redshifts.

4. Matched-filter catalogues

We applied the matched filter algorithm with the parameters determined above to the r'- and z'-band galaxy catalogues of the four deep CFHTLS fields. This resulted in lists of 114 candidates in the r'-band and 247 in z'-band as presented in Tables 4 and 5. Here we present the first five lines of each catalogue with the entire lists being available at the CDS. The tables list: in Col. 1 the cluster name, in Cols. 2 and 3 the right ascension and declination in J2000, in Col. 4 the estimated redshift, in Col. 5 the $\Lambda_{\rm cl}$ richness, in Col. 6 the S/N of the peak value of the detection, in Col. 7 the number of bins where the candidate was detected, in Col. 8 the fraction of lost area within a distance of $1h_{75}^{-1}$ Mpc from the cluster position, in Col. 9 the grade as defined below, and in Col. 10 the corresponding i'-band detection when there is a match. Table 6 gives the 12 matches between r'- and z'-band but not detected in i'.

The effective area covered by the search is 3.112 square degrees and leads to average densities for the four deep fields in r'-band of 36.6 ± 4.3 per square degree with an estimated noise frequency of 11.9 ± 3.6 per square degree and in z' of 79.7 ± 9.1 per square degree with a noise contribution of 20.2 ± 5.4 per square degree. Figure 2 displays the redshift and richness distributions of the detections in the two catalogues. The median redshift is 0.5 for the r'-band detections and 0.8 for the z'-band ones.

With the available multi-passband coverage we created colour images for each of the detected candidates. These images were used for visual inspection in order to obtain a measure of their reliability in terms of their colour and concentration appearance. During the visual inspection grades were assigned from A to D with grade A systems showing a clear concentration of galaxies with similar colours; grade B systems are characterised by an overdensity of galaxies, less concentrated than grade A systems or without any obvious colour concentration; grade C systems do not reveal any clear galaxy overdensity; and finally grade D systems are systems that were detected because of lack of masking of the galaxy catalogue or because of an artefact due to the presence of an edge. The inspection done for this paper was carried out by CB. However, originally when the system was setup, both LFG and CB inspected about half of the cluster candidates. For that sample we estimate that we agreed in ~90% of the cases. In general, the quality of the detected systems is high with about two thirds of the systems in the first two categories. The distribution in r' was found to be grade A 31%, grade B 40%, grade C 29%, and no grade D systems. In z' we found grade A 30%, grade B 36%, grade C 34%, and no grade D systems. In both cases the fraction of systems graded A or B is marginally less than for the i'-band catalogue (Paper I). This may indicate a better success rate of detecting physical systems using the i'-band data, even though this should not be the case judged from the estimated fraction of false detections. This classification is expected to be quantified in a future paper discussing the

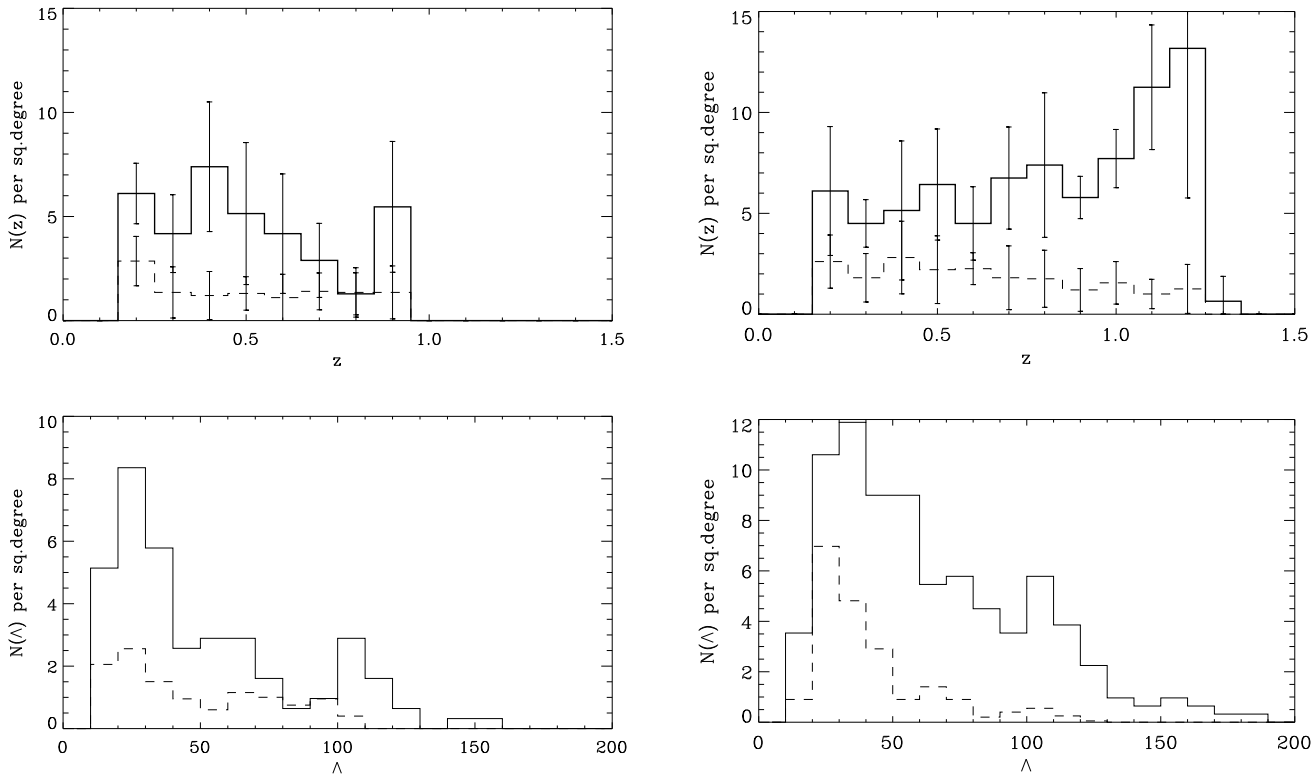

Fig. 2. Redshift (*top*) and richness (*bottom*) distributions (solid line) for all the candidate clusters in the r'- (*left*) and z'-band (*right*) catalogues. The distributions for the false detections (dashed lines) are estimated using the simulated backgrounds described in the text. For the redshift distributions the error bars denote the scatter between the fields.

colour-magnitude diagrams and in particular the red sequence of the detected systems.

5. Value of multiple passbands

In this section we compare the detections identified in r'-, i'-, and z'-band to shed light on how this combination of bands is best used to select the least contaminated samples and how they can be combined for constructing a more complete catalogue. The first question considers candidates detected in multiple passbands (Sect. 5.1), the second those detected in only one band (Sect. 5.2).

Throughout this section, we have to identify those systems we consider the most likely clusters among the candidates. To do so, we follow the procedure introduced in Paper I based on systematic visual inspection. A more robust classification based on photometric redshifts will be presented in a forthcoming paper. The candidates graded A or B both show a concentration of galaxies and thus we consider these the most promising candidates and in this section will be counted as the most likely real systems. It is important to emphasise that when a more thorough investigation becomes available some of the grade C systems may also turn out to be physical systems, just as some of the grade A and B systems may turn out to be false.

The cross-matching between different passbands is made by positional coincidence such that two detections are matched if the centres are within 0.5 Mpc of each other. In practice, this is done by matching the cluster candidates in order of increasing redshift and then identifying other detections within 0.5 Mpc. If more than one detection in the same passband is found to match a given detection, then the one with the closest match in redshift is preferred. If this does not give a unique match, we assign the detection closest in redshift and space as the corresponding candidate. In this way we define a unique matching without a particular reference catalogue.

When interpreting the results of the matching, it is important to keep in mind that not all bands are equally efficient at all redshifts. The bluest band (here r') will become inefficient before the redder ones due to the shift of the 4000 Å break through the filters with increasing redshift. From Sect. 3.4 we see that the r'-band is sensitive to systems of richness class $R \gtrsim 1$ up to $z = 0.5$, while the i'- and z'-bands are sensitive to such systems up to redshifts $z \sim 0.7$. Therefore, in the following these redshifts are used as guides for the discussion of the value of the different bands.

The observing strategy of the CFHTLS is to first complete the i'-band survey. Therefore we chose to use this as a reference in the discussion, even though the matching of the candidates is not related to any particular band. In the following we discuss the matching between the new catalogues and the one based on the i'-band from Paper I. Table 7 summarises the main numbers.

5.1. Selecting the least contaminated sample

In this section we use the candidates matched either between r' and i' or i' and z' to investigate whether these combinations can be used to select samples that are less contaminated than the individual catalogues.

In Sect. 3.4 we found that the r'-band catalogue becomes significantly incomplete at $z \gtrsim 0.5$. Therefore, we concentrate on lower redshifts when discussing the matching between the r'- and i'-band catalogues. In the i'-band catalogue we find

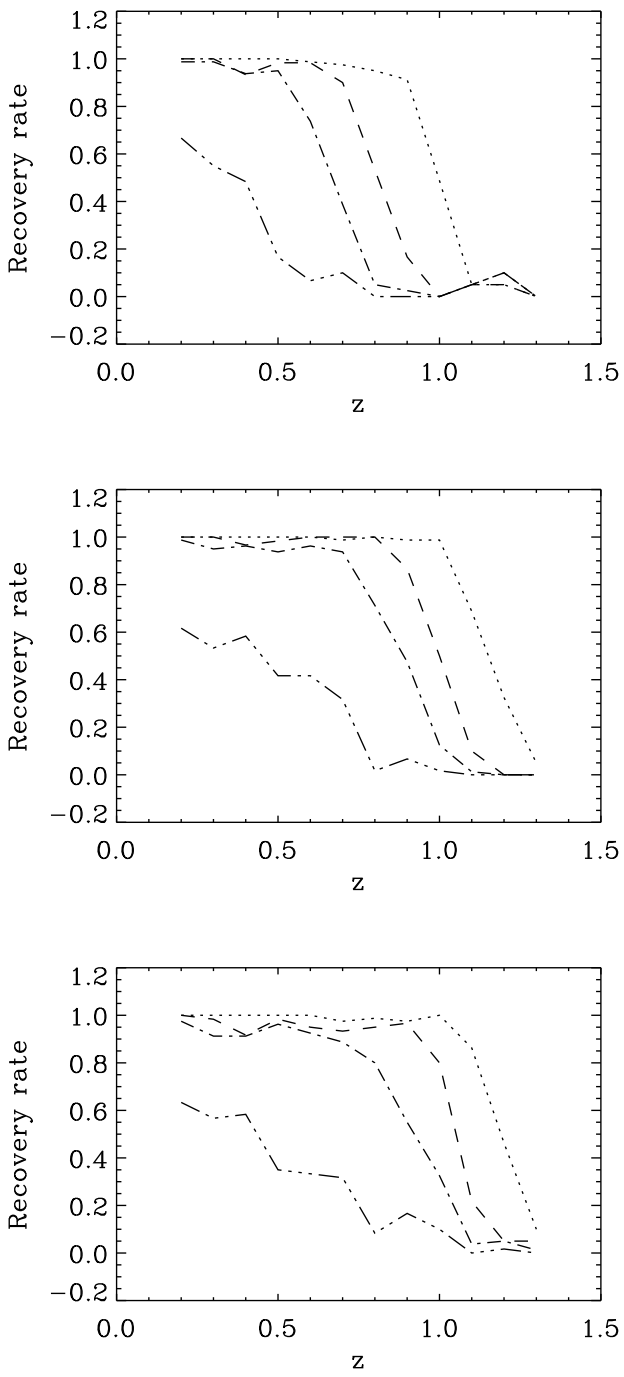

Fig. 3. The recovery rate as derived for each band (*from top to bottom*: r', i' and z') used in the present work. The lines cover different richness classes: $R \lesssim 0$ (triple dot-dashed), $R \sim 1$ (dot-dashed), $R \sim 2$ (dashed), and $R \gtrsim 3$ (dotted).

76 candidates with $z_{i',\mathrm{MF}} \leq 0.5$. Of these, 49 are also detected in the r'-band. The redshift estimates for the candidates in common agree well. The largest offset is $\Delta z = 0.1$ and the mean redshift offset $\langle \Delta z \rangle = -0.01 \pm 0.06$. Also the richness estimates agree well with a mean of $\langle \Delta \Lambda_{\mathrm{cl}} \rangle = 0.5 \pm 11$. We find that of the 76 i'-band candidates ∼82% are graded A or B, while it is ∼88% for the matched sample.

For combining i'- and z'-band we limit the discussion to $z \lesssim 0.7$ corresponding to the redshift where the catalogues become incomplete as seen in Fig. 3. We find 114 candidates with $z_{i',\mathrm{MF}} \leq 0.7$. Of these, 87 are also detected in the z'-band data. The redshift and richness estimates agree well for the matched candidates. We find $\langle \Delta z \rangle = -0.004 \pm 0.06$ and $\langle \Delta \Lambda_{\mathrm{cl}} \rangle = -1.2 \pm 7.9$. The grade distribution for the i'-band candidates show that ∼82% have grades A or B. Among the detections matched with a z'-band candidate the fraction of systems graded A or B is ∼83%. Therefore, we conclude that, in the sense of corroborating the candidates in this redshift range, the z'-band data does not add any significant information.

In Fig. 4 we show the redshift and grade distribution of candidates for the entire i'-band catalogue and matched between the r'- and i'-band and i'- and z'-band. For each set of candidates the distribution is normalized by the total number of candidates in the set, in order to facilitate the comparison of the frequency of the different grades. In general it can be seen that there is a large fraction of systems with grades A or B in all samples and at all redshifts. Furthermore, the grade distributions as a function of redshift are similar for the different samples (i' only, $r' + i'$ and $z' + i'$) except maybe for a slight improvement in the matched sample at high redshift.

From this discussion it appears that the candidate samples matched between two of the bands are indeed marginally less contaminated in particular at high redshift. In deciding whether such a combined sample is preferred over a one-passband sample, it has to be taken into account that the selection function of the combined sample is more complicated than in the single passband case. Therefore, even if the matched samples are less contaminated, it may be preferable to keep the larger more well-understood samples as the basis for many applications.

5.2. Complementing the i'-band catalogue

With data available in several passbands, one can study how the individually extracted catalogues complement each other. In this section, we discuss whether the candidates detected in one passband only (r' or z') represents a significant contribution, relative to the i'-band detections, for constructing a complete cluster sample. We use the quality of the detections in the r'- or z'-band (but not matched with i') to quantify whether these candidates are likely to be an important contribution to a complete cluster sample.

In Fig. 5 we show the redshift and grade distribution for the entire i'-band catalogue together with the same distribution for the candidates detected in r' or z' but without a match in i'-band. It can be seen immediately that the number of r'-band detections without a match in i' is relatively small while in particular at higher redshifts the z'-band contribution may be a significant addition to the i'-band catalogue.

To understand this in more detail, we first concentrate on the r'-band. The total r'-band sample consists of 114 candidates of which a total of 84 match an i'-band candidate. The remaining 30 candidates can be split into 17 with $z_{r',\mathrm{MF}} \leq 0.5$ and 13 with $z_{r',\mathrm{MF}} > 0.5$. In the low-redshift bin the fraction of good candidates is ∼65%, but dominated by grade B cases. In the high-redshift data set, the fraction of good candidates decreases to ∼6%. Including these grade A and B systems in a follow-up programme would increase the sample by ∼10% at the expense of complicating the selection function.

For the z'-band catalogue we first consider detections at redshifts $z_{z',\mathrm{MF}} \leq 0.7$. In total there are 21 systems that were not detected in the i'-band. Of these ∼62% or 13 systems are graded A or B, with about two thirds in the latter category. At these redshifts the addition of the good z'-band candidates to the good

Table 4. The first five entries of the cluster candidate catalogue for the r'-band. The full table is available at the CDS.

Name	α (J2000)	δ (J2000)	z_{MF}	Λ_{cl}	S/N	# Bins	Frac. of lost area	Grade	i'-match
CFHTLS-CL-J022406-041926	02:24:06.2	–04:19:26.8	0.8	100.6	4.35	3	0.41	A	CFHTLS-CL-J022410-041940
CFHTLS-CL-J022411-042510	02:24:11.5	–04:25:10.7	0.9	109.4	3.89	2	0.16	C	CFHTLS-CL-J022411-042511
CFHTLS-CL-J022412-040347	02:24:12.2	–04:03:47.3	0.9	101.3	3.60	2	0.04	B	CFHTLS-CL-J022413-040412
CFHTLS-CL-J022419-040927	02:24:19.5	–04:09:27.7	0.8	106.3	4.59	3	0.37	C	
CFHTLS-CL-J022422-040650	02:24:22.6	–04:06:50.7	0.9	104.2	3.70	2	0.08	C	

Table 5. The first five entries of the cluster candidate catalogue for the z'-band. The full table is available at the CDS.

Name	α (J2000)	δ (J2000)	z_{MF}	Λ_{cl}	S/N	# Bins	Frac. of lost area	Grade	i'-match
CFHTLS-CL-J022410-041931	02:24:10.3	–04:19:31.5	0.9	70.0	4.76	5	0.19	C	
CFHTLS-CL-J022410-041902	02:24:10.7	–04:19:02.4	0.6	33.1	3.68	4	0.20	A	CFHTLS-CL-J022410-041940
CFHTLS-CL-J022411-040323	02:24:11.2	–04:03:23.1	1.0	87.5	4.89	4	0.03	B	CFHTLS-CL-J022413-040412
CFHTLS-CL-J022417-045715	02:24:17.1	–04:57:15.9	1.2	110.6	3.90	2	0.09	C	
CFHTLS-CL-J022423-044044	02:24:23.1	–04:40:44.3	0.4	28.9	4.55	3	0.07	B	CFHTLS-CL-J022423-044044

Table 6. The matches between r'- and z'-band with no i'-band detection.

Name r'-band	Name z'-band
CFHTLS-CL-J022422-040650	CFHTLS-CL-J022423-040648
CFHTLS-CL-J022423-041105	CFHTLS-CL-J022424-041102
CFHTLS-CL-J022616-045621	CFHTLS-CL-J022617-045618
CFHTLS-CL-J100033+024028	CFHTLS-CL-J100034+024034
CFHTLS-CL-J100201+023643	CFHTLS-CL-J100201+023659
CFHTLS-CL-J100205+022359	CFHTLS-CL-J100205+022413
CFHTLS-CL-J141651+524452	CFHTLS-CL-J141651+524448
CFHTLS-CL-J141940+523331	CFHTLS-CL-J141940+523309
CFHTLS-CL-J221450-174956	CFHTLS-CL-J221449-174852
CFHTLS-CL-J221634-173324	CFHTLS-CL-J221634-173308
CFHTLS-CL-J221635-175536	CFHTLS-CL-J221632-175528
CFHTLS-CL-J221721-175947	CFHTLS-CL-J221712-175956

i'-band candidates would increase the sample with ∼14%. At higher redshifts the z'-band catalogue has a lot more candidates than the i'-band, but only ∼24% of these are in the categories of grade A or B. This is a total of 26 candidates, which is comparable to the number of good candidates (30 in total) in the i'-band catalogue at these redshifts. Thus, even though 22 of the additional z'-band candidates are graded B, they are an interesting source for completing a cluster catalogue at these higher redshifts. Using the whole sample will add a lot of grade C systems as well. For follow-up programmes it is thus necessary to either add a large number of less promising systems or rely on visual inspection of all candidates as preparation.

In summary, for using these matched filter cluster samples for cosmological studies relying on statistics and thus good knowledge of the selection function, it would be preferable to stick to the individual catalogues, possibly using both the i'- and z'-band catalogues to have a double check of the results. If one wants to assemble a large sample of clusters for investigating the variety of systems identified by the matched filter, the combined sample would be preferred.

6. Design of high-redshift cluster surveys

The design of large imaging surveys aimed at detecting clusters of galaxies is always a balance of depth and area and possibly of the number of passbands used. The adopted strategy will depend on the desired redshift range to be covered and the requirements for including confirmation like detection in multiple passbands or even the ability to compute photometric redshifts for a more solid confirmation of the detected cluster candidates. In this section we use the available data from the CFHTLS Deep to extract catalogues based on the expected depth of the CFHTLS Wide data to investigate the properties of those wider but shallower catalogues. We will also use the comparison of the deep and shallow catalogues to discuss the best strategy for constructing a matched-filter cluster catalogue at $z \gtrsim 1$.

6.1. Expectations for CFHTLS Wide

The ongoing CFHTLS Wide Survey is planned to cover a total of 170 square degrees of the sky split in 4 different patches[5]. The area will be covered in the 5 Sloan bands (u^*, g', r', i', z') planned to reach limiting magnitudes up to 25^m. We are mainly interested in the high-redshift ($z \gtrsim 1$) cluster population. In the previous section, we saw that the i'- and z'-bands are the relevant ones for such a catalogue, we limit this discussion to these two bands. The currently planned depth for the Wide data is $i' \leq 24.5$ and $z' \leq 23.7$.

As for the Deep data we used simulations to assess the number of false detections and to determine the selection functions. We use the same detection parameters as before, which is the result of the same procedure for assessing the minimum area and detection thresholds as used for the Deep data. To get a realistic prediction for the densities and other general properties of the Wide catalogues we use the Deep data as a basis but execute the cluster search with the shallower limiting magnitudes expected for the Wide galaxy catalogues.

Since in the following, we compare the catalogues with the shallow limiting magnitudes with the deep ones, we list in Table 8 the main properties of the 4 catalogues used in this section. Here, we will first discuss the properties of the shallow catalogues expected to represent the Wide data and below we will return to the comparison with the deeper catalogues.

The candidate density in the shallow catalogues is 50.8 ± 6.4 in i' and 57.6 ± 7.3 in z'. The number of false detections is 16.6 ± 4.8 and 20.2 ± 5.0, respectively. These numbers of false detections correspond to a frequency of false detections of about one third. In the upper panels of Fig. 6 we show the redshift distribution of the detected candidates, together with the redshift

[5] http://terapix.iap.fr/cplt/oldSite/Descart/summarycfhtlswide.html

Table 7. Key numbers for the matching between the new catalogues and the one based on the i'-band from Paper I.

Matching with r'-band at $z_{i',\mathrm{MF}} \leq 0.5$	
i'-detections	76
Fraction of grade A&B	82%
Matched with r'	49
$\langle \Delta z \rangle$	-0.01 ± 0.06
Fraction of grade A&B	88%
Non-matches with $z_{r',\mathrm{MF}} \leq 0.5$	17
With grade A&B	11
Addition to i'-catalogue grade A&B	18%
Matching with z'-band at $z_{i',\mathrm{MF}} \leq 0.7$	
i'-detections	114
Fraction of grade A&B	82%
Matched with z'	87
$\langle \Delta z \rangle$	-0.004 ± 0.06
Fraction of grade A&B	83%
Non-matches with $z_{z',\mathrm{MF}} \leq 0.7$	21
With grade A&B	15
Addition to i'-catalogue grade A&B	13%
Additions at higher redshift	
#detections with $z_{i',\mathrm{MF}} > 0.5$ and grade A&B	76
#detections with $z_{r',\mathrm{MF}} > 0.5$, no i'-match and grade A&B	1
#detections with $z_{i',\mathrm{MF}} > 0.7$ and grade A&B	30
#detections with $z_{z',\mathrm{MF}} > 0.7$, no i'-match and grade A&B	26

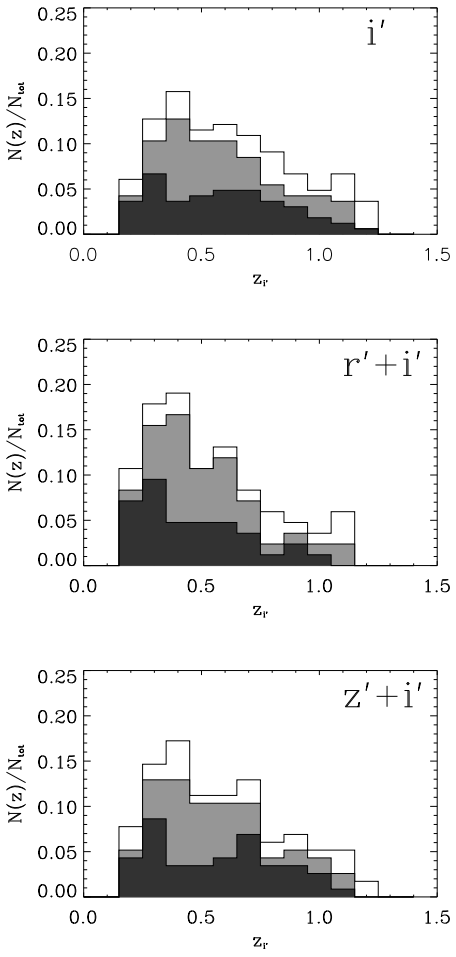

Fig. 4. The i'-band redshift and grade distribution of candidates in the i'-band (*upper panel*) and matched between r'- and i'-band (*middle panel*) and i'- and z'-band (*lower panel*) of all candidates graded A (dark grey), B (light grey) and C (no shading).

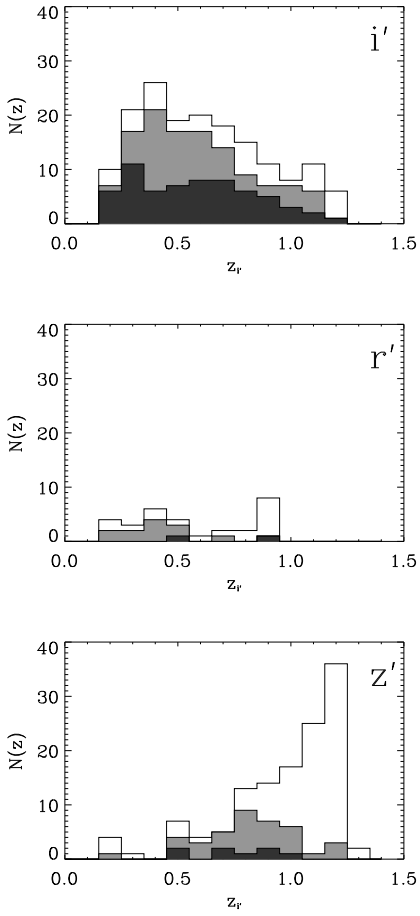

Fig. 5. The i'-band redshift and grade distribution of candidates in the i'-band (*upper panel*). *The middle panel* shows the redshift and grade distributions for systems detected in r' but not in i' and *the lower panel* those detected in z' but not in i'. The shading denotes the different grades as follows: grade A (dark grey), B (light grey), and C (no shading).

Table 8. Main properties of the 4 catalogues used for investigating the added value of the different depths.

Passband	Mag. limit	# Det.	Density	False Dens.	Med. z
i'	24.5	158	50.8 ± 6.4	16.6 ± 4.8	0.6
i'	25.0	169	54.4 ± 7.0	16.9 ± 5.4	0.6
z'	23.7	179	57.6 ± 7.3	20.2 ± 5.0	0.7
z'	24.5	247	79.7 ± 9.1	20.3 ± 5.4	0.8

distribution for the false detections. The errorbars are field-to-field standard deviations. With these results we would expect to detect a total of about 9000 cluster candidates in the complete Wide survey, which when subtracting the expected number of false detections would correspond to a sample of about 6000 real clusters.

As for the deep catalogues, we have carried out a visual inspection of all the candidates included in the shallow catalogues. In Table 9 we summarise the resulting grade distributions. The fraction of systems with grade A or B is slightly smaller in the z'-band catalogue than in the i'-band. We have matched the candidates between the shallow i'- and z'-band catalogues. The matching is carried out as in Sect. 5. We find 109 candidates detected in both catalogues. As can be seen from the table the grade distribution of this sample has a marginally higher fraction of grade A or B systems than both of the individual catalogues, but also the selection function of the sample is more complicated to estimate. Looking at the complementary 70 systems included in the z'-band catalogue but without a counterpart in i'-band, we find that the fraction of A or B systems is only 47%, thus at first sight this subsample is more contaminated than any other subsample. The z'-band is, however, expected to add most to the high-redshift end where the 4000 Å break shifts out of the i'-filter. Therefore we also include the statistics for systems with $z \geq 0.7$. For this redshift range, the total number of detections in i'-band is 59 (43 with grades A or B) including matched and non-matched detections. Out of the 59 systems, 38 were found in both catalogues with 31 (82%) systems having grades A or B, thus a slightly higher fraction than for the i'-band sample. For the systems found in z'- but not in i'-band, we find that 26 (50%) are in these grade categories. Thus even though the fraction of good grade systems is not as impressive, addition of the z'-band detections will increase the size of the sample of promising candidates by about 60%. At the same time, it also increases the number of less promising (grade C) systems from 16 to 42, thus an increase of about 150%. For any application the final decision on whether to use the samples separately or combined will depend on the scientific aim. From this we conclude that the z'-band is a significant contribution towards a more complete high-z sample, even though with the drawback of adding a relatively large number of less promising systems.

6.2. Comparing Deep and Wide catalogues

An important question in designing imaging surveys for cluster searches is how to balance the observing time between different bands. Here we use the available Deep catalogues and compare them with the Wide equivalent catalogues to discuss the value of deeper i'- and z'-band data for the construction of a matched-filter cluster catalogue reaching $z \gtrsim 1$.

Table 8 gives the general properties of the four catalogues in question. It can be seen that for the i'-band the additional depth in the deep catalogue does not add much in terms of additional detections, while in the z'-band the candidate density is increased dramatically. Turning to the number density of false detections, it can be seen that the differences are very small with an insignificant increase of not even one detection per square degree.

Table 9. Grade distributions of candidates in the shallow catalogues upper part refers to all candidates and the lower half for the high-redshift sample with $z \geq 0.7$.

Catalogue	A	B	C	D
i'-band	60 (38%)	63 (40%)	35 (22%)	0 (0%)
z'-band	53 (30%)	69 (39%)	56 (31%)	1 (<1%)
i'- and z'-band	46 (42%)	43 (40%)	20 (18%)	0 (0%)
i'-band only	14 (29%)	20 (41%)	15 (31%)	0 (0%)
z'-band only	7 (10%)	26 (37%)	36 (52%)	1 (1%)
$z \geq 0.7$				
i'-band	22 (37%)	21 (36%)	16 (27%)	0 (0%)
z'-band	25 (28%)	32 (36%)	33 (36%)	0 (0%)
i'- and z'-band	20 (52%)	11 (29%)	7 (18%)	0 (0%)
i'-band only	2 (10%)	10 (48%)	9 (42%)	0 (0%)
z'-band only	5 (10%)	21 (40%)	26 (50%)	0 (0%)

In Fig. 6 the redshift distributions of the candidates in the four different catalogues are compared. For the i'-band the distributions are not very different, which is consistent with the number of candidates being increased by only 11 (∼7%) between the shallow and the deep catalogues. For the z'-band, the situation is very different. Here the deeper catalogue has a large increase at the high-redshift end.

The difference in the number of detections originate in both the differences in limiting magnitude and in wavelength of the filters. For the i'-band the 0.5 mag depth difference between the two catalogues roughly corresponds to the difference in apparent Schechter magnitude between two adjacent shells corresponding to a redshift difference of 0.1. The difference is 0.8 mag for the z'-band and more closely corresponds to the offset in apparent Schechter magnitude for a redshift difference of 0.2, thus twice as large as for the i'-band. This in itself would lead to an increase in the number of detections in the z'-band relative to the i'-band. The other effect, the different wavelength intervals covered by the filters, leads to the shifting of the 4000 Å break through the i'-band wavelengths for lower redshifts than for the z'-band. In fact, the 4000 Å break has shifted completely out of the i'-band filter at $z \sim 1.1$, where it starts moving through the z'-band filter. Therefore, the z'-band catalogue is likely including intrinsically fainter galaxies than the i'-band allowing for detection of poorer systems, which in turn may correspond to the grade C systems seen in the catalogue.

A better quantification of the value of deeper data to construct cluster catalogues can be obtained from investigations of the systems detected either only in the shallow or only in the deep catalogue in the same band. To identify these detections we carried out a matching for the catalogues extracted from the same band. Again, the matching is carried out as in Sect. 5. For the i'-band the overlap is very large with 146 detections in both catalogues or alternatively only 12 detections in the shallow catalogue not in the deep and 23 in the deep not in the shallow. In the z'-band, there are 155 detections in common and 24 detections in the shallow catalogue that were not found in the deep and 91 in the deep not in the shallow. The large number of detections in the deep catalogues not in the shallow is due, for both bands (though more pronounced in z' than in i'), to additional high redshift detections. The quality of the detections is important for assessing the differences between the catalogues. Therefore, Table 10 gives the grade distributions for the

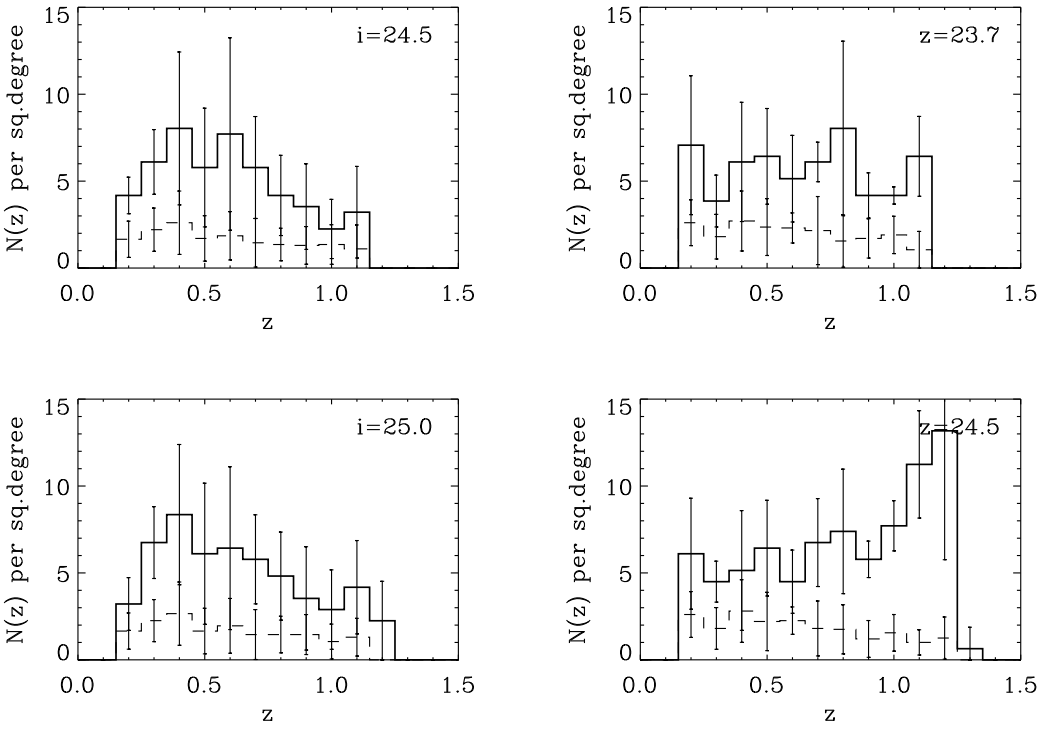

Fig. 6. The redshift distribution for the candidates (solid line) and false detections (dashed lines) for the two magnitude limits and the two passbands as indicated in each panel. The error bars are field to field standard deviations.

detections found in either a shallow or a deep catalogue. For the i'-band we find that the number of promising candidates is the same in the two catalogues (in both the shallow and deep catalogue 9 systems are graded A or B), but the actual systems are different. In addition, the number of less promising systems in the deep catalogue is larger than in the shallow one. For the z'-band the number of promising candidates in the deep catalogue is slightly higher (18) than for the shallow catalogue (12). The number of grade C systems is much greater in the deep z'-band catalogue than in any of the others. In all cases most of the unmatched detections are found at redshifts $z \geq 0.7$, which is even more pronounced for the deep than for the shallow catalogues. From this we conclude that the depth of the z'-band catalogue is important for building a complete cluster sample at redshifts $z \sim 1$, though controlling purity remains an issue.

7. Summary

We applied the matched-filter detection technique to the CFHTLS Deep data in the r'- and z'-bands with limiting magnitudes of $25^{\rm m}$ and $24.5^{\rm m}$, respectively. These catalogues are compared with that of the i'-band with a limiting magnitude of $25^{\rm m}$ presented in Paper I. The density of detections in r'-band is 36 ± 4 and in z'-band 80 ± 9. The estimated fraction of noise is 33% in r'-band and 25% in the z'-band catalogues. Selection functions are derived based on simple simulations and show that the r'-band catalogue starts to become significantly incomplete at redshifts $z \gtrsim 0.5$, where only clusters in Abell richness classes $R \geq 2$ are recovered at more than 80%. For the z'-band catalogue, the corresponding redshift limit is $z \gtrsim 0.7$ and the most distant systems have redshifts beyond 1.

The constructed catalogues are compared with the one extracted from the i'-band data and presented in Paper I. The comparison is used to investigate the gain in terms of added leverage of the samples based on a combination of bands and in terms of additional detections missed in one of the bands. Using a grading based on a visual inspection of colour images of all the candidates, we conclude that the visual appearance of candidates detected in more than one band is not more promising than for the one-band samples individually. This result we attribute to the way the matched filter handles the background and cluster model. Since one of the main properties of a group of galaxies to enter into the catalogue is its concentration, the same concentration of galaxies is likely to appear in all bands. In terms of complementing the samples in i'-band, we find that the r'-band contribution is insignificant, while the candidates detected in z'-band are a significant contribution to the i'-band sample.

We also used the data to investigate what to expect for cluster extraction in the ongoing CFHTLS Wide survey. This is accomplished by restricting the search for clusters to the planned limiting magnitudes of $i' \leq 24.5$ and $z' \leq 23.7$. With these numbers we find densities of 51 and 58 detections per square degree in i' and z', respectively, with estimated noise fraction of 33% in both cases. From these numbers we estimated a total number of detections from the completed wide catalogues of about 9000 with about 6000 of these corresponding to clusters. Also in this case we compared the visual appearance of the detections in the two catalogues and find results similar to the deep case, i.e. the matched samples appear as promising as the individual ones. Furthermore, the z'-band data are important for complementing the i'-band catalogue at $z \geq 0.7$, increasing the number of candidates by ~60%.

Finally, we investigate the impact in terms of detections and quality by decreasing the depth from the Deep to the Wide limiting magnitudes. For the i'-band the difference between the two catalogues is insignificant, while for the z'-band a large number

Table 10. Grade distributions of candidates in either a shallow or a deep catalogue.

Catalogue	A	B	C	D
Shallow i' not deep	3 (25%)	6 (50%)	3 (25%)	0 (0%)
Deep i' not shallow	6 (26%)	3 (13%)	10 (43%)	4 (17%)
Shallow z' not deep	3 (13%)	9 (37%)	12 (50%	0 (0%)
Deep z' not shallow	4 (4%)	14 (15%)	70 (77%)	3 (3%)

of systems is missed in the shallower case. Therefore, when planning future matched filter cluster searches for clusters at $z \gtrsim 1$ it may be preferable to increase the depth in z' and keep the i'-band relatively more shallow, at least when reaching depths comparable to the ones discussed here.

Acknowledgements. We thank the anonymous referee for useful comments that helped improving the paper. The work was based on observations obtained with MegaPrime/MegaCam, a joint project of CFHT and CEA/DAPNIA, at the Canada-France-Hawaii Telescope (CFHT), which is operated by the National Research Council (NRC) of Canada, the Institut National des Science de l'Univers of the Centre National de la Recherche Scientifique (CNRS) of France, and the University of Hawaii. This work is based in part on data products produced at TERAPIX and the Canadian Astronomy Data Centre as part of the Canada-France-Hawaii Telescope Legacy Survey, a collaborative project of NRC and CNRS. L.F.G. acknowledges financial support from the Danish Natural Sciences Research Council and the Poincaré fellowship programme at the Observatoire de la Côte d'Azur. The Dark Cosmology Centre is funded by the Danish National Research Foundation.

References

Bahcall, N., McKay, T., Annis, J., et al. 2003, ApJS, 148, 243
Borgani, S., Rosati, P., Tozzi, P., et al. 2001, ApJ, 561, 13
Bower, R., Lucey, J., & Ellis, R. 1992, MNRAS, 254, 601
de Propris, R., Stanford, S. A., Eisenhardt, P. R., Dickinson, M., & Elston, R. 1999, AJ, 118, 719
Gavazzi, R., & Soucail, G. 2007, A&A, 462, 459
Gladders, M., & Yee, H. 2000, AJ, 120, 2148
Gladders, M., & Yee, H. 2005, ApJS, 157, 1
Goto, S., Nichol, B. L, Kim, A., et al. 2002, AJ, 123, 1807
Kepner, J., Fan, X., Bahcall, N., Gunn, J., & Lupton, R. 1999, ApJ, 517, 78
Kim, R., Kepner, J., Postman, M., et al. 2002, AJ, 123, 20
Koester, B. P., McKay, T. A., Annis, J., et al. 2007, ApJ, 660, 221
Mazure, A., Adami, C., Pierre, M., et al. 2007, A&A, 467, 49
Miller, C. J., Nichol, R. C., Reichart, D., et al. 2005, AJ, 130, 968
Olsen, L. F., Scodeggio, M., da Costa, L., et al. 1999a, A&A, 345, 681
Olsen, L. F., Scodeggio, M., da Costa, L., et al. 1999b, A&A, 345, 363
Olsen, L. F., Benoist, C., Cappi, A., et al. 2007, A&A, 461, 81 (Paper I)
Popesso, P., Böhringer, H., Romaniello, M., & Voges, W. 2005, A&A, 433, 415
Postman, M., Lubin, L., Gunn, J., et al. 1996, AJ, 111, 615
Postman, M., Lauer, T., Oegerle, W., & Donahue, M. 2002, ApJ, 579, 93
Rosati, P., della Ceca, R., Norman, C., & Giacconi, R. 1998, ApJ, 492, L21
Rosati, P., Borgani, S., & Norman, C. 2002, ARA&A, 40, 539
Schechter, P. 1976, ApJ, 203, 297
Schlegel, D., Finkbeiner, D., & Davis, M. 1998, ApJ, 500, 525
Scodeggio, M., Olsen, L. F., da Costa, L., et al. 1999, A&AS, 137, 83
Stanford, S., Eisenhardt, P., & Dickinson, M. 1998, ApJ, 492, 461